HTS Detector Magnet Demonstrator Based on a 3D-Printed Partially-Insulated Support Cylinder

Joep L. Van den Eijnden, Anna K. Vaskuri, Benoit Curé, Alexey Dudarev, and Matthias Mentink

***Abstract*—In this work, we extend the experimental demonstration of partially-insulated, ultra-radiation transparent detector magnet technology based on a 3D-printed aluminium alloy support structure containing 10% of silicon. This demonstrator magnet has a bore diameter of 390 mm, effective wall thickness of 3.7 mm, and it has 15 turns corresponding to 19 meters of HTS conductor. The HTS conductor of the magnet consists of a stack of four ReBCO tapes with a width of 4 mm. We measured the magnet to be fully superconducting at 4.2 K with an operating current of 4.5 kA. A time constant of the magnetic field delay to a current step measured was 83 s. This detector magnet technology may be used in future particle detector magnets, such as the AMS-100 solenoid, where one of the key design requirement is a passive self-protection by partial-insulation which ensures continuous operation and stable magnetic field even with a locally damaged conductor.**

***Index Terms*—Al10SiMg, aluminium-stabilized, detector magnet, HTS magnet, HTS, partial insulation, ReBCO, radiation transparent, self-protected, ultra-thin, 3D-printing.**

I. Introduction

We have developed a high temperature superconducting (HTS) demonstration coil within the CERN EP R&D project on Experimental Detector Magnets. The magnet builds upon recent experimental demonstration of aluminium-stabilised HTS conductors [1], [2] and a demonstrator magnet [3], [4] and supports the development of an ultra-radiation transparent HTS solenoid for the space-borne AMS-100 particle detector [5].

For particle detectors in which the magnet is situated between the interaction point and the calorimeter, there is a requirement for radiation transparency, achievable by employing aluminium as a stabiliser for the superconductor. Aluminium has a low density and thus high radiation transparency [6] while having high thermal and electrical conductivity. The largest particle detector magnets in the world, ATLAS and CMS, are made from Nb–Ti Rutherford cables stabilised using pure aluminium [7], [8]. In this work, an HTS demonstrator magnet is developed, taking a step towards experimentally validating the use of the high-temperature superconductor ReBCO in particle detector magnets. The utilisation of ReBCO as a conductor offers the highest current density among all high-temperature superconductors, while enabling operation at elevated temperatures. This is advantageous not only in response to the current and anticipated helium shortage [9], [10] but also for specific projects like AMS-100, where detector magnet operation above 50 K is a requirement [5].

Numerous ReBCO magnets have been built for fusion and high-field applications [11], [12], [13]. The first HTS pancake coil without turn-to-turn insulation was reported in 2011 [14]. However, as far as the authors are aware, no functional HTS magnet for particle detectors incorporating aluminium stabilisation, apart from our smaller earlier prototype [3], has been developed. The combination of ReBCO, aluminium stabilisation and partial insulation makes this magnet technology distinctive.

AMS-100's magnet design consists of the combination of the three aforementioned technologies and should be self-protected by it. An understanding of the transient behaviour of such a magnet is essential before construction can start. The only way to verify simulations is to build prototypes, incrementally increasing in size, to validate the behaviour of this coil technology while at the same time advancing manufacturing techniques. Changes from our last demonstrator magnet [3] encompass the size, thus stored energy, and improved current-leads. Not only are the overall mass of the solenoid and the electrical contact resistance lower, but the improved current-leads do not form a ring which could give rise to significant edge-effects while studying transient behaviour, allowing more resembling quench studies to be done in the future.

The coil has a stored magnetic energy of 1.3 kJ at 4.5 kA, ten times higher than our first demonstrator in [3], and it consists of an additive manufactured aluminium alloy (Al10SiMg) cylinder acting both as a stabiliser for the superconductor and mechanical support. The structure makes the coil partially insulated and self-protected against quenches, provided that good local cooling can be maintained, but it comes at the price of a higher boil-off rate and limited ramp-rate as the current will start flowing in the axial direction before redistributing to the helical path of the coil. Earlier, we successfully characterized a smaller 230 mm diameter open-bore coil featuring five turns and a stack of four REBCO tapes (4 mm wide, Fujikura FESC-SCH04) from 4.2 K to 77 K [3]. The HTS coil presented in this work extends the developed novel technology, soldering ReBCO tapes to a

Manuscript received 19 September 2023; revised 10 January 2024 and 28 January 2024; accepted 14 February 2024. Date of publication 27 February 2024; date of current version 14 March 2024. This work was supported by CERN EP R&D on Experimental Technologies (WP8 Detector Magnets). (*Corresponding author: Joep L. Van den Eijnden.*)

Joep L. Van den Eijnden is with the Eindhoven University of Technology, 5612 AE Eindhoven, The Netherlands, and also with CERN, 1211 Geneva, Switzerland (e-mail: jvde99@gmail.com).

Anna K. Vaskuri, Benoit Curé, Alexey Dudarev, and Matthias Mentink are with CERN, 1211 Geneva, Switzerland.

Color versions of one or more figures in this article are available at https://doi.org/10.1109/TASC.2024.3370125.

Digital Object Identifier 10.1109/TASC.2024.3370125

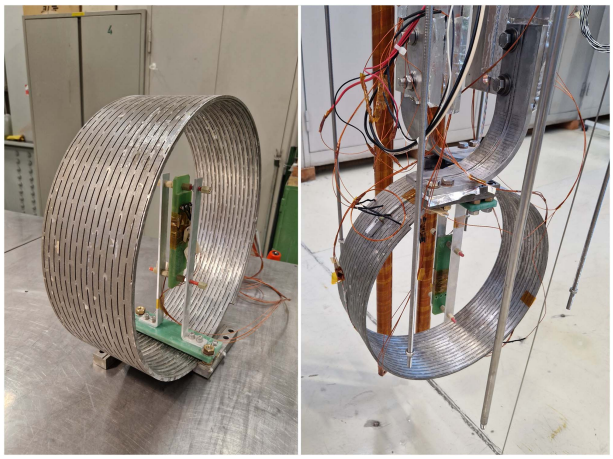

Fig. 1. HTS detector magnet demonstrator with a bore diameter of 390 mm (a) and the magnet assembled in the cryostat insert for characterization measurements (b).

TABLE I
PROPERTIES OF THE 390 MM OPEN-BORE HTS MAGNET

Design parameter	Value (at 4.5 kA)	Unit
	Conductor	
Conductor	4 ReBCO tapes soldered to Al10SiMg U-profile	
Aluminium alloy	3D-printed Al10SiMg	
HTS type	Fujikura FESC-SCH04	
Solder	tin-lead (Sn–Pb)	
	Coil	
Inner diameter	390	mm
Length	127.5	mm
Number of shorts per turn	32	[-]
Width of short	3.1	mm
Thickness of cylinder wall	5	mm
Effective thickness of cylinder wall	3.7	mm
Depth groove in U-profile	2	mm
Weight coil and copper terminals	3	kg
Inductance (15 turns)	0.124	mH
N_{turns}	15	[-]
Central B-field	0.2	T
Peak B-field on conductor	1.3	T
Stored magnetic energy	1.3	kJ
Energy density	0.4	kJ/kg

U-shaped groove of a 3D-printed aluminium cylinder, on a larger scale and we report the design with measured characteristics at 4.2 K and 77 K.

II. DESIGN

The HTS magnet demonstrator developed in this work and presented in Fig. 1 has 15 turns, a bore diameter of 390 mm, and is designed to produce 0.2 T central magnetic field at 4.5 kA and 4.2 K with a peak field of 1.35 T on the HTS conductor. The coil has a stored magnetic energy of 1.3 kJ. The properties of the HTS coil are listed in Table I.

The coil consists of a 3D-printed aluminium cylinder that acts as aluminium stabilisation, provides partial insulation, and gives mechanical support to the tape-stack. The cylinder features a helical groove on the inside, where the ReBCO tapes are soldered to. There are holes in between the turns of the helical groove. In between the holes, each turn is connected to the adjacent turns by

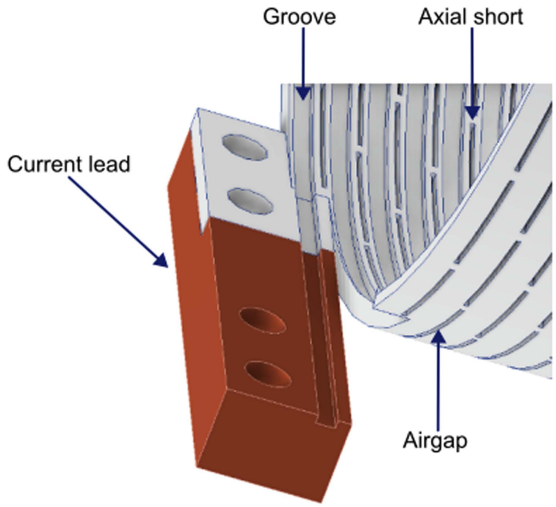

Fig. 2. Drawing of the aluminium cylinder and a copper current lead. The groove on the inside of the cylinder extends into the current lead, and the holes in the cylinder provide partial insulation between turns.

axial shorts, as depicted in Fig. 2. The dimensions and quantity of the shorts determine the resistance between turns, and thus the transient behaviour. We chose to keep these quantities similar to our previous coil, as these also have an effect on the mechanics of the support structure.

We aimed to reduce the heat load on the 390 mm bore HTS coil compared to our earlier 230 mm bore coil in [3] by placing oxygen-free electronic copper terminals at the entrance and exit of the HTS helix of the coil as shown in Fig. 2. The copper terminals have a groove that aligns with the helical groove in the inner side of the cylinder. The four ReBCO tapes were soldered inside the groove using tin-lead solder in a staircased pattern. Staircased means that each tape is positioned overlapping the one beneath it, providing a direct contact area of 4×20 mm with the terminal. The magnet is soldered in an oven where a Teflon tube is used to press the tapes inside the groove during the soldering process, similar as described in [1], [2]. The copper terminals reduce the contact resistance and thus heat load during operation.

The ring-shaped current leads of our last prototype, as described in [3], could act as a bypass for the current and thermal sink in case of a quench. These newly designed leads are expected to cause fewer edge effects and achieve a higher energy density, better resembling the final scale coils.

The coil features nine voltage taps, dividing the coils in eight sections across which the voltage can be independently measured. In addition, two voltage taps are located on the copper current-leads, allowing for a measurement of contact losses when compared to the voltage taps placed on the superconducting coil. The simulated maximum Von Mises stress in the cylinder at 4.5 kA is 36 MPa, which lies well within the yield strength of 3D-printed Al10SiMg of 300 MPa stated by the manufacturer (IN3DTEC).

III. RESULTS

We ramped up the magnet to 4420 A, limited by the power-supply, while it was submerged in liquid helium and waited

TABLE II
COMPARISON OF SIMULATED AND MEASURED VALUES OF THE CENTRAL MAGNETIC FIELD, TIME CONSTANT OF THE MAGNETIC FIELD RESPONSE TO A CURRENT STEP, AND INDUCTANCE OF THE 14 CENTRAL TURNS OF THE HTS MAGNET. UNCERTAINTIES ARE GIVEN AT 2σ LEVEL

	Measured	Simulated using [15]	Difference
Central B-field	(0.198 ± 0.005) T	0.198 T	0%
Inductance (14 turns)	(103 ± 4) μH	109 μH	5.5%
Time constant (B-field)	(83 ± 4) s	90 s	7.8%

for the magnetic field to stabilize. The central magnetic field and inductance measured are compared to the results simulated using [15] in Table II. The corresponding electric and central magnetic field measurements as function of current are shown in Fig. 3(a). Additionally, the magnetic field as function of time is shown in Fig. 3(b) and voltage across the 14 central turns in Fig. 3(c), respectively. The shown measurement was not the first ramp-up after cooling-down to 4.2 K. At the beginning of this measurement, a remnant field from the previous ramping cycle can be observed due to what we believe is a persistent current flowing in a loop formed by spilled superconducting tin-lead solder shortening the turns via the axial shorts.

When ramping up, a delay in the rise of the magnetic field and induced voltage with respect to the ramping current be observed in Fig. 3(b)–(c) respectively. The voltage stays at zero for more than five minutes, then peaks, and gradually stabilises to a constant value, corresponding to the inductance of the coil. In parallel, the magnetic field remains constant during the initial ramp-up, increases significantly, and then experiences a decrease in rate, coinciding with the behaviour of the induced voltage. The observed behaviour of the magnetic field and induced voltage arises possibly from eddy screening currents created by ReBCO and superconducting tin-lead in the same loops that keep the persistent current and give rise to the remnant field. At currents above ~3 kA, the effect has vanished and the coil behaves as expected for a partially-insulated coil.

To see how the HTS magnet behaves when the critical current of the HTS conductor is exceeded, we also measured the current-to-electric field curve across 14 turns and current-to-magnetic field curve at 77 K. These results are plotted in Fig. 4. As the critical current of the HTS conductor is exceeded, current starts redistributing via axial shorts which can be seen as simultaneous plateauing of the central magnetic field and increasing voltage across the magnet. Therefore, the transition edge of the current-to-electric field measured is linear corresponding to the magnet's axial resistance of ~920 nΩ across 14 turns. No remnant field or effects of shielding eddy currents are observed since tin-lead is not superconducting at 77 K.

The response of the magnet to a step down to zero current was measured at 77 K for a range of initial currents as depicted in Fig. 5. The responses are fitted to an exponential decay function to find the magnetic time constant equal to (83 ± 4) s with 2σ uncertainty. It agrees within 8% with the estimated time constant $\tau = L/R \approx 90$ s obtained using the simulated inductance L and axial resistance R of the coil.

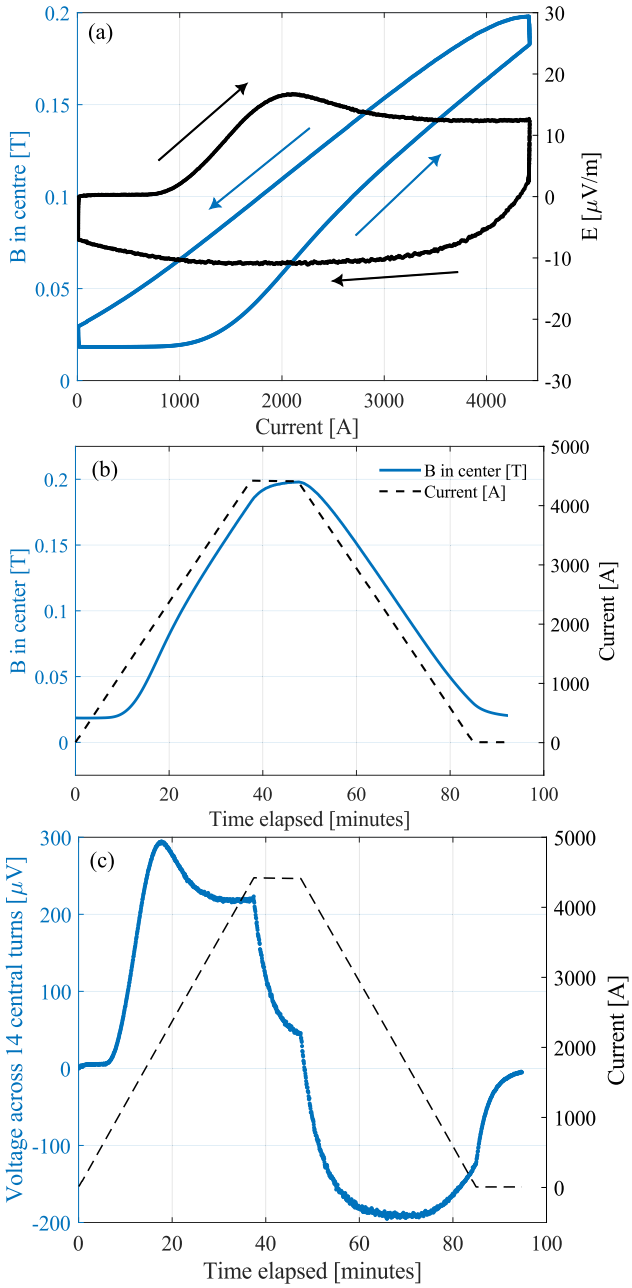

Fig. 3. Current-to-electric field curve and central magnetic field of the HTS magnet measured at a 2 A/s ramp rate at 4.2 K (a). The corresponding delay in central magnetic field and voltage across 14 turns are shown in (b) and (c).

Soldering of the staircased ReBCO tapes directly to the OFE copper terminals of this HTS magnet reduced the heat load compared to our 230 mm bore magnet in [3] where the four ReBCO tapes were staircased and soldered directly to the coated Al10SiMg cylinder by a factor three. The contact resistance between the HTS magnet and the HTS busbars was measured at 4.2 K to be (53.7 ± 1.9) nΩ, which corresponds to 1.1 W of heating at 4.5 kA. This way we were able to reduce the contact resistance by a factor of three compared to that of the 230 mm bore magnet.

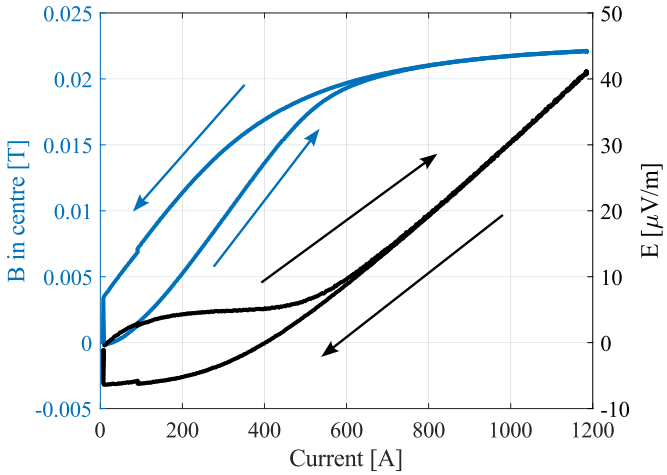

Fig. 4. Current-to-electric field curve and central magnetic field of the HTS magnet measured at a 1 A/s ramp rate at 77 K. Note that, after ramping the magnet down, both the magnetic and electric field converge to zero after several magnetic time constants τ.

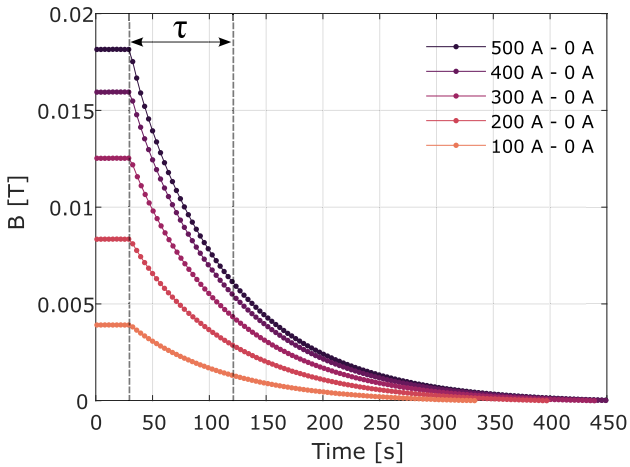

Fig. 5. Exponential decay response of the magnetic field to a step down in current at 77 K, and magnetic time constant τ.

IV. Conclusion

In this work we present the measured characteristics of the HTS detector magnet demonstrator at 77 K and 4.2 K. The HTS magnet has a bore diameter of 390 mm and 15 turns, which is equivalent to 19 meters of an HTS conductor.

The magnet features a stack of four ReBCO tapes and it was measured to be fully superconducting at 4.2 K and 4.5 kA. The measured time constant of magnetic field delay is 83 s. This extends the experimental demonstration of partially insulated aluminium-stabilised HTS coils which may be used in future particle detector magnets, such as the AMS-100 solenoid.

The connection design of this HTS magnet, where the four staircased ReBCO tapes are connected to oxygen-free electronic copper end pieces, decreases the heat loss at junction by a factor three compared to that of our previously reported 230 mm bore magnet [3]. These current leads are expected to reduce edge effects and increase energy density, making this demonstrator coil more representative of the final scale magnets. This magnet enables more accurate experimental studies of the transient behaviour of partially-insulated solenoid technology to be carried out in the future.

References

[1] A. Vaskuri, B. Curé, A. Dudarev, and M. Mentink, "Aluminium-stabilized high-temperature superconducting cable for particle detector magnets," *IEEE Trans. Appl. Supercond.*, vol. 33, no. 5, Aug. 2023, Art. no. 4500506.

[2] A. K. Vaskuri, J. L. V. d. Eijnden, B. Curé, A. Dudarev, and M. Mentink, "Characteristics of aluminium-stabilized HTS detector magnet cable at 4 K and 5 T," in *IEEE Trans. Appl. Supercond.*, doi: 10.1109/TASC.2024.3369570.

[3] J. L. Van den Eijnden, A. K. Vaskuri, B. Curé, A. Dudarev, and M. Mentink, "Self-protected high-temperature superconducting demonstrator magnet for particle detectors," *Supercond. Sci. Technol.*, vol. 37, 2024, Art. no. 015007.

[4] J. L. Van den Eijnden, "Two self-protected HTS demonstration coils for particle detectors," M.S. thesis, Eindhoven Univ. Technol., Eindhoven, The Netherlands, 2023. [Online]. Available: https://research.tue.nl/en/studentTheses/59c3f277-2c58-4af6-9487-072fb16d6a62

[5] S. Schael et al., "AMS-100: The next generation magnetic spectrometer in space - An international science platform for physics and astrophysics at lagrange point 2," *Nucl. Instrum. Methods Phys. Res. Sect. A: Accel., Spectrometers, Detect. Assoc. Equip.*, vol. 944, 2019, Art. no. 162561.

[6] M. Gupta, "Calculation of radiation length in materials," CERN, Meyrin, Switzerland, Tech. Rep. PH-EP-Tech-Note-2010-013, 2010.

[7] H. H. Ten Kate, "Superconducting magnet system for the ATLAS detector at CERN," *IEEE Trans. Appl. Supercond.*, vol. 9, no. 2, pp. 841–846, Jun. 1999.

[8] I. L. Horvath et al., "The CMS conductor," *IEEE Trans. Appl. Supercond.*, vol. 10, no. 1, pp. 395–398, Mar. 2000, doi: 10.1109/77.828256.

[9] P. B. de Sousa, T. Koettig, U. Wagner, and R. van Weelderen, "Cryogenic options for the muon collider," in *Proc. 1st Annu. Muon Collider Collaboration Meeting*, CERN, Meyrin, Switzerland, Oct. 2022, p. 5. [Online]. Available: https://indico.cern.ch/event/1175126/

[10] F. Ferrand on behalf of the CERN Cryogenics Group, "Helium medium & long term availability," in *Proc. 4th Supercond. Magnet Test Stands Workshop*, Salerno, Italy, Apr. 2023, pp. 16–20. [Online]. Available: https://agenda.infn.it/event/32061/

[11] S. Hahn et al., "45.5-tesla direct-current magnetic field generated with a high-temperature superconducting magnet," *Nature*, vol. 570, pp. 496–499, 2019.

[12] T. Lécrevisse, X. Chaud, P. Fazilleau, C. Genot, and J.-B. Song, "Metal-as-insulation HTS coils," *Supercond. Sci. Technol.*, vol. 35, 2022.

[13] Z. S. Hartwig et al., "The SPARC toroidal field model coil program," *IEEE Trans. Appl. Supercond.*, vol. 34, no. 2, Mar. 2024, Art. no. 0600316, doi: 10.1109/TASC.2023.3332613.

[14] S. Hahn, D. K. Park, J. Bascuñán, and Y. Iwasa, "HTS pancake coils without turn-to-turn insulation," *IEEE Trans. Appl. Supercond.*, vol. 21, pp. 1592–1595, 2011.

[15] J. L. Van den Eijnden, A. Vaskuri, and M. Mentink, "ReBCO partially insulated solenoid simulation," *version 1.0*, Nov. 2023. [Online]. Available: https://github.com/JoepVdE/RePISoSi